$(Sr_3N_x)E$ and $(Ba_3N_x)E$ (E = Sn, Pb): Preparation, Crystal Structures, Physical Properties and Electronic Structures

Frank Gäbler, Martin Kirchner, Walter Schnelle, Miriam Schmitt, Helge Rosner and Rainer Niewa*

Dresden/Germany, Max-Planck-Institut für Chemische Physik fester Stoffe

Received August 4th, 2004.

Dedicated to Professor Heinrich Oppermann on the Occasion of his 70th Birthday

Abstract. Black powders of $(Sr_3N_x)Sn$ (x = 0.74(2), a = 523.51(5) pm), $(Ba_3N_x)Sn$ (x = 0.62(2), a = 552.93(1) pm), $(Sr_3N_x)Pb$ (x = 0.81(3), a = 524.22(1) pm) and $(Ba_3N_x)Pb$ (x = 0.826(4), a = 554.40(3) pm, $Pm\bar{3}m$, No. 221, Z = 1) were obtained from reactions of melt beads of the respective metals with bulk compositions of A_3E (A = Sr, Ba; E = Sn, Pb) in nitrogen atmosphere at temperatures in the range of 970 K − 1220 K. The compositions were derived from chemical analyses, supported by Rietveld refinements based on powder X-ray and neutron diffraction patterns taken on $(Ba_3N_x)Sn$ (x = 0.64(1); neutron diffraction: R_{Bragg} = 8.70 %, R_F = 6.10 %; X-ray diffraction: R_{Bragg} = 11.60 %, R_F = 12.00 %). The phases crystallize in cubic anti-perovskite type arrangements. Measurements of the magnetic susceptibility indicate a nearly temperature independent paramagnetism. The electrical resistivities are weakly temperature dependent with resistivities at 300 K in the order of 1 mΩ·cm. Electronic structure calculations on ordered superstructures of the composition $(A_3N_{2/3})E$ reveal the phases as intrinsic metals and suggest the tendency towards higher nitrogen site occupation ($x > {}^2/_3$).

Keywords: Nitrides; Crystal structure; Magnetic susceptibility; Electrical resistivity; Electronic structure calculation

$(Sr_3N_x)E$ und $(Ba_3N_x)E$ (E = Sn, Pb): Darstellung, Kristallstrukturen, physikalische Eigenschaften und elektronische Strukturen

Inhaltsübersicht. $(Sr_3N_x)Sn$ (x = 0,74(2), a = 523,51(5) pm), $(Ba_3N_x)Sn$ (x = 0,62(2), a = 552,93(1) pm), $(Sr_3N_x)Pb$ (x = 0,81(3), a = 524,22(1) pm) und $(Ba_3N_x)Pb$ (x = 0,826(4), a = 554,40(3) pm, $Pm\bar{3}m$, No. 221, Z = 1) wurden als schwarze Pulver durch Reaktion von Schmelzperlen der Zusammensetzung A_3E (A = Sr, Ba; E = Sr, Ba) mit Stickstoff bei Temperaturen im Bereich von 970 K − 1220 K erhalten. Die Zusammensetzungen wurden über chemische Analysen bestimmt und stehen in Übereinstimmung mit Ergebnissen aus Rietveld-Verfeinerungen an Röntgen- und Neutronen-Pulverbeugungsdiagrammen von $(Ba_3N_x)Sn$ (x = 0,64(1); Neutronenbeugung: R_{Bragg} = 8,70 %, R_F = 6,10 %; Röntgenbeugung: R_{Bragg} = 11,60 %, R_F = 12,00 %). Alle Phasen kristallisieren als kubische anti-Perowskite. Messungen der magnetischen Suszeptibilitäten belegen nahezu temperaturunabhängiges paramagnetisches Verhalten. Die elektrischen Widerstände sind schwach temperaturabhängig mit Werten bei 300 K in der Größenordnung von 1 mΩ·cm. Berechnungen der elektronischen Struktur an geordneten Überstrukturen der Zusammensetzung $(A_3N_{2/3})E$ charakterisieren die beschriebenen Phasen als intrinsische Metalle. Die Ergebnisse der Rechnungen deuten auf eine Tendenz zu höheren Stickstoffgehalten ($x > {}^2/_3$).

Introduction

The field of ternary nitrides has been a vivid and fast growing research area in solid state chemistry within the last two decades, as manifested in a multitude of recent reviews [e.g. 1−3]. Cubic anti-perovskite nitrides with the general formula $(Ca_3N)E$ (E = Tl, Ge, Sn, Pb, Sb, Bi, Au; E = P, As distorted to an orthorhombic crystal structure) are already known for a couple of years [4−7]. Recently, we described the cubic anti-perovskites $(Sr_3N)E$ (E = Sb, Bi), and the hexagonal anti-perovskites $(Ba_3N)E$ (E = Sb, Bi) [8]. Earlier, respective Mg compounds $(Mg_3N)E$ (E = As, Sb) were reported [9]. This class of compounds shows an interesting spectrum of electronic situations: Provided ionic counting, $(Ca_3N)Au$ (formal $(Ca^{2+})_3N^{3-}Au^- \cdot 2e^-$) exhibits an electron excess and metallic properties [4], the compounds $(A_3N)E$ (E = P^{3-}, As^{3-}, Sb^{3-}, Bi^{3-}) [5] obey the octet rule and are insulators or semiconductors, while $(Ca_3N)Tl$ ($(Ca^{2+})_3N^{3-}Tl^{3-}$) is an electron deficient metal [6]. Corresponding oxides are only known with group 14 elements $(A_3O)E$ (A = Ca, Sr, Ba; E = Si, Ge, Sn, Pb) and consequently may be obtained as colorless insulators [10−13]. The analogous anti-perovskite nitrides $(Ca_3N)E$ with E = Sn, Pb remarkably are reported to exhibit nearly temperature independent electrical resistivities [5]. These facts and the electronic and structural properties have raised considerable interest in theoretical studies of the electronic structures and high pressure investigations of the crystal structures of alkaline-earth metal anti-perovskite nitrides

* Dr. R. Niewa
Max-Planck-Institut für Chemische Physik fester Stoffe
Nöthnitzer Str. 40
D-01187 Dresden
Fax: +49 (0) 351 4646 3002
e-mail: niewa@cpfs.mpg.de

 DOI: 10.1002/zaac.200400344

[6, 14−18]. Electronic structure calculations on $(Ca_3N)Pb$ indicated a strong peak in the density of states (DOS) directly at the Fermi energy (E_F), which was taken as an indication for a structural distortion, but such a distortion could not be validated by experimental data.

Only few ternary nitrides with E = Sn, Pb are known. Previously reported were the cubic anti-perovskites $(Ca_3N)E$ [5], $(Nd_3N)E$ [19], $(Cr_3N)Sn$ [20], $(Mn_3N)Sn$ [20], $(Mn_3N)Mn_{0.5}Sn_{0.5}$ [21], and $(Fe_3N)Fe_{0.4}Sn_{0.6}$ [22], the filled Mn_5Si_3 type $(Zr_3N)Zr_2Sn_3$ [23] and the filled Cr_5B_3 type $(La_4N)LaPb_3$ [24]. Ternary nitrides with tin or lead and A = Sr, Ba are not known so far.

Experimental

All manipulations were carried out in an argon filled glove box ($p(O_2, H_2O)$ < 1 ppm). For the preparation of single phase samples tin or lead (Chempur 99.999 %) and strontium or barium (Alfa Aesar, 99.9 %) were fused in an arc furnace (molar ratio 1 : 3, typically 2 − 4 g total sample mass) operated in argon (Messer-Griesheim, 99.999 %, additionally purified by passing over molsieve, Roth 3 Å, and BTS-catalyst, Merck). No binary phases A_3E with A = Sr, Ba and E = Sn, Pb are known according to the phase diagrams [25]. The samples consisted of the phases A_2E and A according to X-ray powder diffraction. In a second step the metallic regulus was heated in nitrogen of ambient back-pressure (Messer-Griesheim, 99.999 %, additionally purified as described for argon) to maximum temperatures of T = 1170 K (Sr−Sn), T = 970 K (Ba−Sn), T = 1220 K (Sr−Pb), and T = 1120 K (Ba−Pb). This approach leads to better results compared with solid state sinter reactions of binary nitrides AN_x with melt beads A_xE of appropriate compositions in Ar atmosphere. The reaction temperatures were taken from DTA/TG experiments: e. g., melt beads of the bulk compositions A_3Sn in nitrogen atmosphere increased in weight up to T = 1250 K (Sr) and T = 1000 K (Ba). Above these temperatures the weight decreased substantially. All four ternary nitrides were obtained as grayish-black powders, which are sensitive against water and moisture.

Chemical analyses were carried out using the carrier gas hot-extraction technique on a LECO analyzer TCH-600. Quantitative analyses of A and Sn were performed using an ICP-OES (Varian Vista RL). All values are averages of at least 3 independent measurements. These measurements led to the following bulk compositions:

w(Sr) = 66.3(2) %, w(Sn) = 27.8(4) %, w(N) = 2.62(6) %, w(O)= 0.16(1) %, i. e. $(Sr_{3.00(1)}N_{0.74(2)}O_{0.04(1)})Sn_{0.93(1)}$
w(Ba) = 77.1(8) %, w(Sn) = 21.9(6) %, w(N) = 1.64(4) %, w(O) = 0.19(2) %, i. e. $(Ba_{3.00(3)}N_{0.62(2)}O_{0.064(5)})Sn_{0.98(3)}$
w(Sr) = 52.5(4) %, w(Pb) = 43.3(2) %, w(N) = 2.26(4) %, w(O)= 0.19(6) %, i. e. $(Sr_{3.00(2)}N_{0.81(3)}O_{0.06(2)})Pb_{1.046(4)}$
w(Ba) = 66(1) %, w(Pb) = 32(1) %, w(N) = 1.85(1) %, w(O) < 0.10 %, i. e. $(Ba_{3.00(6)}N_{0.826(4)})Pb_{0.96(1)}$

DTA/TG-measurements were performed on a STA 449C (Ar- or N_2-atmosphere purified as described above, thermocouple type S, NETZSCH Gerätebau, Selb, Germany) completely integrated into a glove box to avoid hydrolysis reactions. Temperature calibration was obtained using 5 melting standards in the temperature range from 370 K to 1470 K.

The ternary nitrides were characterized by X-ray powder diffraction using an Imaging Plate Guinier Camera (HUBER diffraction, CuKα_1 radiation, 4×15 min scans, 8° ≤ 2θ ≤ 100°). The samples were loaded between two polyimide foils in an aluminium cell with a rubber sealing to exclude moisture.

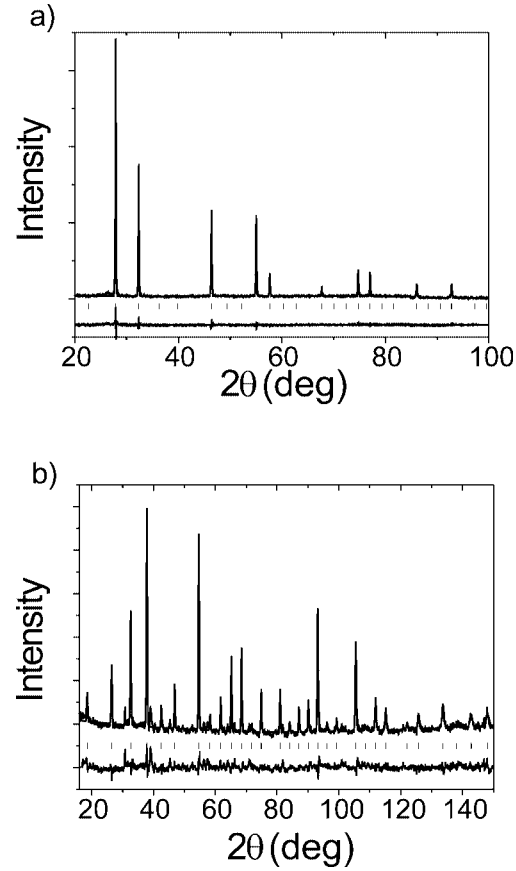

Figure 1 a) X-ray powder diffraction pattern and b) neutron diffraction pattern of $(Ba_3N_{0.64(1)})Sn$. The measured data are shown as points, the continuous line represents the calculated profile and the lower line shows the difference between the calculated and observed intensities. The marks below the data indicate the positions of the reflections.

Neutron powder diffraction data on the microcrystalline sample of $(Ba_3N_x)Sn$ were gathered at the E9 powder diffractometer at BERII, HMI Berlin, Germany. The sample was contained in a gas-tight vanadium cylinder (diameter 6 mm, lengths 51 mm, wall thickness 0.15 mm). The structure was refined simultaneously on the basis of both powder X-ray diffraction and neutron diffraction patterns. Figure 1 depicts the experimental diffraction patterns (fig. 1a: X-ray diffraction, fig. 1b: neutron diffraction) together with the calculated profiles and the difference curves of the observed and the simulated patterns as determined by least squares refinements (program package FULLPROF [26]). Additional peaks only visible in the neutron diffraction pattern are due to a small admixture of an unknown impurity phase. In X-ray diffraction patterns of the sample taken prior and after the neutron diffraction experiment no indication for a second phase was apparent.

The magnetization data of powder samples (sealed in silica tubes, 400 mbar He) were measured in a SQUID magnetometer (MPMS XL-7, Quantum Design) in external magnetic fields ranging from 70 kOe to 20 Oe between 1.8 K and 400 K. Corrections for small ferromagnetic impurities were applied for the $(Sr_3N_x)Pb$ data.

Measurements of the electrical resistivity were performed on powders pressed in a sapphire die in a four contact dc van-der-Pauw set-up between 4 K and 320 K.

Calculations

To investigate the electronic structure of the phases $(Sr_3N_x)E$ and $(Ba_3N_x)E$ (E = Sn, Pb) a full potential non-orthogonal local-orbital scheme (FPLO) [27] within the local density approximation (LDA) was applied. In the scalar relativistic calculations we used the exchange and correlation potential of *Perdew* and *Wang* [28]. To simulate a nitrogen content close to $x = {}^2/_3$, a 3-fold tetragonal supercell with the content of $(A_9N_2)E_3$ (space group $P4/mmm$, $a_{tet} = a_{cub}$, $c_{tet} = 3a_{cub}$) was constructed, with one N site in the center of the supercell unoccupied to obtain the nominal composition $(A_3N_{2/3})E$. As basis set N(2*s*,2*p*,3*d*), Sr(4*s*,4*p*,5*s*,5*p*,4*d*), Ba(5*s*,5*p*,6*s*,6*p*,5*d*), Sn(4*s*,4*p*,4*d*,5*s*,5*p*,5*d*) and Pb(5*s*,5*p*,5*d*,6*s*,6*p*,6*d*) states were taken into account. The lower lying states were calculated as core states that are treated fully relativistically. The N(3*d*), Sr(4*d*), Ba(5*d*) as well as the Pb(6*d*) states were considered as polarization states to increase the completeness of the basis set. The inclusion of the Sr(4*s*,4*p*), Ba(5*s*,5*p*), Sn(4*s*,4*p*,4*d*) and Pb(5*s*,5*p*,5*d*) semi-core like states in the valence was necessary to account for non-negligible core-core overlaps. The spatial extension of the basis orbitals, controlled by a confining potential [29] was optimized to minimize the total energy. A **k**-mesh of 63 points in the irreducible part of the Brillouin zone of the 3-fold tetragonal supercell was used to ensure accurate density of states and band structure information. All calculations have been carried out for the experimentally observed unit cell dimensions and atomic positions.

Results and Discussion

The optimal preparation conditions for ternary nitrides $(A_3N_x)E$ (A = Sr, Ba; E = Sn, Pb) from mixtures of the metals or their binary compounds in nitrogen atmosphere were derived from extensive DTA/TG investigations. These DTA/TG measurements on melt beads of the bulk composition 'A_3E' in nitrogen atmosphere already indicated the uptake of less than one equivalent N per 'A_3E' composition. According to the TG curves of the reaction of 'Sr_3Sn' with nitrogen (heating rate 10 K/min) a significant weight gain starts at a temperature of T = 793 K, increases appreciably at a temperature that probably represents the eutectic temperature of the system Sr−Sr_2Sn at T = 992 K (endothermal effect), and is completed at about T = 1270 K. The weight gain of $\Delta m/m$ = 2.52 % corresponds to an uptake of ${}^2/_3$ equivalents N per 'Sr_3Sn'. Similarly, for 'Ba_3Sn' samples the weight gain accelerates at a temperature of T = 799 K accompanied by a broad exothermal effect (this temperature might be correlated with the eutectic temperature of the system Ba−Ba_2Sn, whereby the heat of reaction may outweigh the endothermal melting effect), and is completed at about T = 970 K. The weight gain of $\Delta m/m$ = 2.00 % is intermediate between the uptake of ${}^2/_3$ equivalents N per 'Ba_3Sn' ($\Delta m/m$= 1.76 %) and the formation of $(Ba_3N)Sn$ ($\Delta m/m$= 2.64 %). This DTA/TG measurement is exemplarily depicted in figure 2. For the corresponding Pb systems the TG curves show a more complicated behavior with several steps, but similarly, the weight increases considerably above T = 770 K and the complete weight increase is only slightly above the values expected for a composition of $(A_3N_{2/3})Pb$ (Sr: $\Delta m/m$ = 2.06 %, expected for ${}^2/_3$ equivalents N were $\Delta m/m$ = 1.99 %, for 1 equivalent N $\Delta m/m$ = 2.98 %; Ba: $\Delta m/m$ = 1.58 %, expected for ${}^2/_3$ equivalents N $\Delta m/m$ = 1.51 %, for 1 equivalent N $\Delta m/m$ = 2.26 %). The reaction products from DTA/TG experiments showed X-ray powder diffraction patterns consistent with cubic anti-perovskite crystal structures and typically no or only small reflections due to impurity phases. Obviously, the ternary nitrides represent stable compounds in nitrogen atmosphere at the reaction temperature.

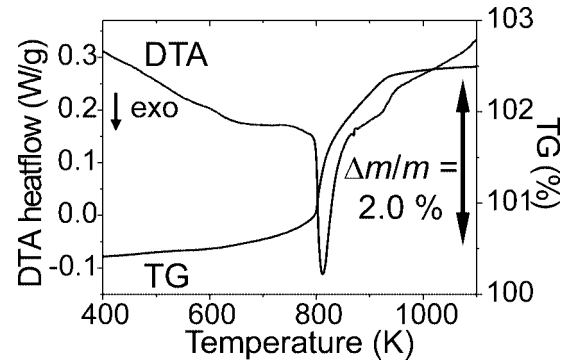

Figure 2 Simultaneous DTA/TG measurement of the reaction of melt beads of the general composition of 'Ba_3Sn' with nitrogen (heating rate 10 K/min) forming $(Ba_3N_x)Sn$.

The title compounds adopt anti-perovskite type arrangements ($Pm\bar{3}m$, No. 221, Z = 1) with nitrogen in octahedral coordination by six alkaline-earth metal ions and tin in the resulting voids of this framework, as also known from, e. g., the isotypes $(Ca_3N)E$ with E = P, As, Sb, Bi; Ge, Sn, Pb; Tl [5, 6]. The following unit cell parameters were obtained: $(Sr_3N_x)Sn$, x = 0.74(2): a = 523.51(5) pm, $(Ba_3N_x)Sn$, x = 0.62(2): a = 552.93(1) pm, $(Sr_3N_x)Pb$, x = 0.81(3): a = 524.22(1) pm and $(Ba_3N_x)Pb$, x = 0.826(4): a = 554.40(3) pm (the nitrogen content x was derived from the chemical analyses results). For the Sn containing phases distances d(Sn−Sr) = 370.18(3) pm are longer than those in SrSn [30]: d(Sn−Sr) = 344 pm − 361 pm, Sr_2Sn [31]: d(Sn−Sr) = 334 pm − 400 pm and Sr_5Sn_3 [32]: d(Sn−Sr) = 340 pm − 357 pm. Similar, distances d(Sn−Ba) = 390.98(2) pm are longer than those in BaSn [30]: d(Sn−Ba) = 364 pm − 373 pm, Ba_2Sn [31]: d(Sn−Ba) = 357 pm − 419 pm and Ba_5Sn_3 [32]: d(Sn−Ba) = 359 pm − 378 pm. Distances d(Sr−N) = 261.76(3) pm and d(Ba−N) = 276.97(1) pm are only slightly longer compared to those in subnitrides with nitrogen species in octahedral coordination: Sr_2N (261 pm) [33] and Ba_3N (273 pm) [34]. The corresponding distances for the Pb containing phases are: $(Sr_3N_x)Pb$, d(Pb−Sr) = 370.68(1) pm (Sr_2Pb: d(Pb−Sr) = 335 − 401 pm [31]), d(N−Sr) = 262.11(1) pm; $(Ba_3N_x)Pb$, d(Pb−Ba) = 392.02(2) pm (Ba_2Pb: d(Pb−Ba) = 347 − 420 pm [31]), d(N−Ba) = 277.20(2) pm. No indications for a distortion from cubic

Table 1 Results of Rietveld refinements of X-ray and neutron powder diffraction data on $(Ba_3N_x)Sn$.

	X-ray diffraction	neutron diffraction
No. of structural parameters	4	4
Radiation	Cu$K\alpha_1$	1.797977(9)
Unit cell parameters a [pm]	552.918(8)	
Rietveld		
Unit cell parameters a [pm]	552.93(1)	
Guinier		
Space group	$Pm\bar{3}m$, No. 221	
Occupation and displacement parameters:		
Ba	B_{iso} = 2.65(7) $\times 10^{-4}$ pm^2	
Sn	B_{iso} = 1.7(1) $\times 10^{-4}$ pm^2	
N	B_{iso} = 1.0(1) $\times 10^{-4}$ pm^2, x = 0.64(1)	
$R_{profile}$, R_{Bragg}	0.120, 0.116	0.061, 0.087

metric could be obtained from X-ray powder diffraction patterns. Distortions of the cubic unit cell to an othorhombic one (space group *Pnma*) were observed for the comparably small species of P and As in combination with Ca−N frameworks [5], and for analogous oxides with Si and Ge [10, 13].

The joint Rietveld refinements of a neutron powder diffraction pattern and the corresponding X-ray powder diffraction pattern of $(Ba_3N_x)Sn$ resulted in a N site occupation of x = 0.64(1) (neutron diffraction: R_{Bragg} = 8.70 %, R_F = 6.10 %; X-ray diffraction: R_{Bragg} = 11.60 %, R_F = 12.00 %, compare data in table 1), consistent with the composition from chemical analyses: $(Ba_{3.00(3)}N_{0.62(2)}O_{0.064(5)})Sn_{0.98(3)}$. Although the neutron diffraction pattern shows two impurity reflections of unknown origin (2θ = 30.94°, 39.14°) while X-ray diffraction patterns of the sample taken prior and after the neutron diffraction experiment did not indicate any second phase, together with the results of the chemical analyses and in the light of the electrical resistivity data discussed below, an idealized composition of $(Ba_3N_{2/3})Sn = (Ba_9N_2)Sn_3$ can be assumed. Such a composition would be in accordance with the octet rule: $(A^{2+})_3(N^{3-})_{2/3}E^{4-}$. Additionally, the phases under discussion are able to incorporate some excess N leading to a homogeneity range in the sense of $(A_3N_{2/3+x})E$ (or $(A_3N_{1-x})E$, respectively). Especially, the possibility of partial occupancy of the N site is in contrast to all previous reports on $(A_3N)E$ phases (E = main-group element, A = Mg, Ca, Sr, Ba), where experimental evidence pointed at full occupancy (or was assumed, if no experimental evidence from structure refinements on suitable diffraction data or chemical analyses was available), but connects to the relations in $(R_3N_{1-x})E$ phases (R = rare-earth metal). Such rare-earth metal phases can tolerate substantially lower nitrogen contents than unity (i. e., $x \geq 0$), depending on the chemical system [35].

The temperature dependencies of the magnetic susceptibility of the four phases (figure 3) can be interpreted as the sums of diamagnetic core contributions χ_{dia}, weakly temperature dependent Pauli-paramagnetic terms and minor paramagnetic impurities with Curie behavior. Extrapol-

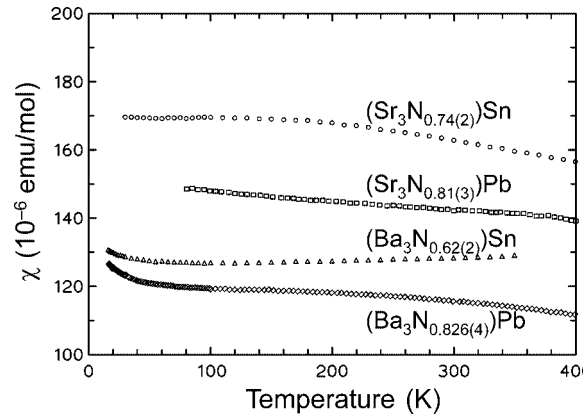

Figure 3 Magnetic susceptibilities of phases $(A_3N_x)E$ with A = Sr, Ba and E = Sn, Pb as function of temperature.

Table 2 Results of the fitting of magnetic susceptibility measurements (10^{-6} emu/mol) and calculated electronic density of states $D(E_F)$ (states/eV per formula unit)

Phase	χ_0	χ_{dia} [36]	$\chi_0-\chi_{dia}$	$D(E_F)$
$(Sr_3N_{0.74(2)})Sn$	+169(5)	−73	+242	7.5
$(Sr_3N_{0.81(3)})Pb$	+150(20)	−83	+233	7.2
$(Ba_3N_{0.62(2)})Sn$	+126(5)	−124	+250	7.7
$(Ba_3N_{0.826(4)})Pb$	+116(5)	−134	+250	7.7

ations with the expression $\chi(T) = C/T + \chi_0 + \chi_1 T + \chi_2 T^2$ to T = 0 K yield the constant χ_0. The values for χ_0 and ($\chi_0 - \chi_{dia}$) are gathered in table 2 (diamagnetic core increments used are $\chi_{dia}(Sr^{2+}) = -15 \times 10^{-6}$ emu/mol, $\chi_{dia}(Ba^{2+}) = -32 \times 10^{-6}$ emu/mol, $\chi_{dia}(Sn^{4+}) = -16 \times 10^{-6}$ emu/mol, $\chi_{dia}(Pb^{4+}) = -26 \times 10^{-6}$ emu/mol, $\chi_{dia}(N^{3-}) = \chi_{dia}(O^{2-}) = -12 \times 10^{-6}$ emu/mol [36]). The resulting ($\chi_0 - \chi_{dia}$) indicate quite similar electronic densities of states at the Fermi level for all four phases of about $D(E_F) \approx 7.5$ states/eV.

Figure 4 shows the electrical resistivities of powder samples of the compounds under consideration. Besides residual resistivities between 0.2 and 1.2 mΩ·cm the samples (except $(Ba_3N_{0.62(2)})Sn$) display a metallic temperature characteristic with $\rho(300\ K) - \rho_0 \approx 0.4 - 0.6$ mΩ·cm. $\rho(T)$ for $(Ba_3N_{0.62(2)})Sn$ is almost independent of temperature. Similar behavior is known from ternary inter-transition metal nitrides [37−39].

The densities of states (DOS) resulting from electronic structure calculations carried out on ordered three-fold superstructures with the idealized composition $(A_9N_2)E_3$, i. e., $(A_3N_{2/3})E$ are shown in figure 5. For these compositions the phases can be described according to the octet rule, $(A^{2+})_9(N^{3-})_2(E^{4-})_3$, and therefore might be expected to exhibit semiconducting properties. However, all calculations result in metallic behavior with values of 4 to 5 states/eV per formula unit $(A_3N_{2/3})E$ for the density of states at the Fermi level. This is in qualitative agreement with the experimental observations from the susceptibility measurements, justifying a posteriori the choice of the simple supercell.

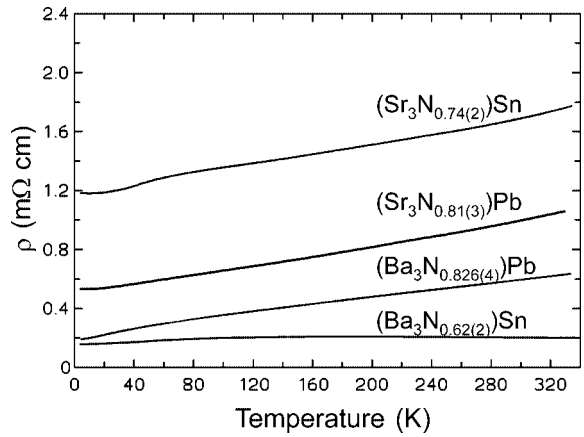

Figure 4 Electrical resistivities of phases $(A_3N_x)E$ with A = Sr, Ba and E = Sn, Pb as function of temperature.

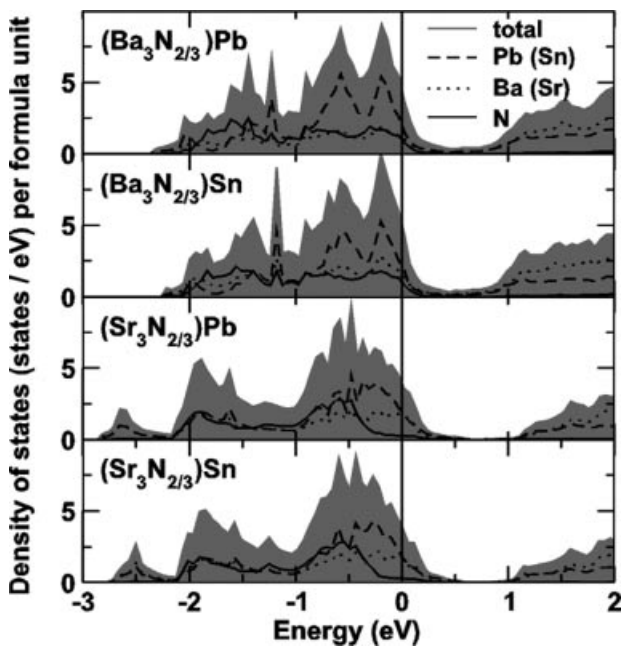

Figure 5 Total and partial density of states per formula unit for $(Ba_3N_{2/3})Pb$, $(Ba_3N_{2/3})Sn$, $(Sr_3N_{2/3})Pb$, and $(Sr_3N_{2/3})Sn$. The Fermi level is located at zero energy.

Comparing the calculated DOS for the investigated compounds with data previously obtained for $(Ca_3N)Bi$ [6], the deep lying rather localized N(2*s*) states are almost unchanged, whereas the Sn(5*s*) (Pb(6*s*)) states are shifted upwards in energy by about 4 eV (not shown) and therefore start to mix into the valence band. Like in $(Ca_3N)Bi$, the main contribution to the valence band stems from N(2*p*), Sn(5*p*) (Pb(6*p*)) and Sr(4*d*) (Ba(5*d*)) states. These states strongly hybridize with each other in the energy region below the Fermi level down to about −2.5 eV. The conduction band is mainly made up from Sr(4*d*) (Ba(5*d*)) states.

A remarkable feature is the occurrence of a region with low DOS (pseudogap; Ba compounds) or zero DOS (gap; Sr compounds) right above the Fermi level (0.5 to 1 eV). Integrating the DOS from the Fermi level to the begin of the (pseudo)gap yields an electron count of about $^1/_3$ electron. In a rigid band approach, this would correspond to the addition of about $^1/_9$ N per formula unit (only the 2*p* electrons take part in the formation of the valence band, the N(2*s*) electrons form a narrow, isolated band at about −11 eV as mentioned above). In turn, such additional N sums up to a composition of about $(A_3N_{0.78})E$, well in accordance with the experimental data. However, the interpretation in terms of a rigid band model has to be taken with great care, because of the strong hybridization of the N(2*p*) states with the Sn(5*p*) (Pb(6*p*)) and the Sr(4*d*) (Ba(5*d*)) states.

The results of the present calculations can not be understood in terms of the octet rule, which would lead to insulating behavior for a composition $(A_3N_{2/3})E$ and consequently to the interpretation of heavily doped semiconductors for the investigated compounds. In contrast, the calculations propose intrinsic metallic behavior, although the influence of the N content and disorder on the charge carrier concentration and the possible localization of charge carriers can not be estimated at the present stage. A more detailed study of the influence of the N concentration and the disorder itself on the electronic structure is required, using an ensemble of larger supercells or a more sophisticated method like the coherent potential approximation (CPA).

In summary, the ternary alkaline-earth nitrides $(A_3N_x)E$ with A = Sr, Ba and E = Sn, Pb crystallize in the cubic perovskite structure type and exhibit nitrogen deficiency compared to full occupation of all sites. Results from magnetic susceptibility and electrical resistivity measurements were related with composition deviations from an ideal formulation according to the octet rule. Electronic structure calculations using a simple ordered three-fold supercell result in metallic properties for the idealized composition $(A_3N_{2/3})E$ and suggest a possible interpretation for the observed compositions.

Acknowledgements. We thank *Steffen Hückmann* for the collection of the diffraction data, *Anja Völzke* for performing the chemical analyses, *Ralf Koban* for operating the SQUID and performing the resistivity measurements, and *Prof. Dr. Rüdiger Kniep* for his constant interest and support. The neutron diffraction data collection by *Dr. Gudrun Auffermann* at the E9 diffractometer operated by *Dr. Daniel Többens* is gratefully acknowledged.

References

[1] R. Niewa, H. Jacobs, *Chem. Rev.* **1996**, *96*, 2053.
[2] R. Kniep, *Pure Appl. Chem*. **1997**, *69*, 185.
[3] R. Niewa, F. J. DiSalvo, *Chem. Mater*. **1998**, *10*, 2733.
[4] J. Jäger, D. Stahl, P. C. Schmidt, R. Kniep, *Angew. Chem*. **1993**, *105*, 738; *Angew. Chem. Int. Ed*. **1993**, *32*, 709.
[5] M. Y. Chern, D. A. Vennos, F. J. DiSalvo, *J. Solid State Chem.* **1992**, *96*, 415.
[6] R. Niewa, W. Schnelle, F. R. Wagner, *Z. Anorg. Allg. Chem.* **2001**, *627*, 365.
[7] M. Y. Chern, F. J. DiSalvo, J. B. Parise, J. A. Goldstone, *J. Solid State Chem*. **1992**, *96*, 426.

[8] F. Gäbler, M. Kirchner, W. Schnelle, U. Schwarz, M. Schmitt, H. Rosner, R. Niewa, *Z. Anorg. Allg. Chem*. **2004**, *630*, 2292.
[9] E. O. Chi, W. S. Kim, N. H. Hur, D. Jung, *Solid State Commun.* **2002**, *121*, 309.
[10] B. Huang, J. D. Corbett, *Z. Anorg. Allg. Chem.* **1998**, *624*, 1787.
[11] A. Widera, H. Schäfer, *Mater. Res. Bull.* **1980**, *15*, 1805.
[12] C. Röhr, *Z. Kristallogr.* **1995**, *210*, 781.
[13] R. Türck, Ph D Thesis, Universität Stuttgart, Germany, 1996.
[14] P. R. Vansant, P. E. Camp, V. E. Van Doren, J. L. Martins, *Phys. Status Solidi B* **1996**, *198*, 87.
[15] D. A. Papaconstantopoulos, W. E. Pickett, *Phys. Rev. B* **1992**, *45*, 4008.
[16] P. R. Vansant, P. E. Van Camp, V. E. Van Doren, J. L. Martins, *Phys. Rev. B* **1998**, *57*, 7615.
[17] P. R. Vansant, P. E. Van Camp, V. E. Van Doren, J. L. Martins, *Comp. Mater. Sci.* **1998**, *10*, 298.
[18] I. R. Shein, A. L. Ivanovskii, *Russ. J. Inorg. Chem*. **2003**, *48*, 711; *Zh. Neorg. Khim.* **2003**, *48*, 801.
[19] H. Haschke, H. Nowotny, F. Benesovsky, *Monatsh. Chem*. **1967**, *98*, 2157.
[20] M. Nardin, G. Lorthioir, M. M. Barberon, R. Madar, E. Fruchart, R. Fruchart, *Compt. Rend. Hebd. Acad. Sci. C* **1972**, *274*, 2168.
[21] M. Mekata, *J. Phys. Soc. Jpn.* **1962**, *17*, 796.
[22] Z. J. Zhao, D. S. Xue, F. S. Li, *J. Magn. Magn. Mater*. **2001**, *232*, 155.
[23] K. Young-Uk, J. D. Corbett, *Chem. Mater.* **1992**, *4*, 1348.
[24] A. M. Guloy, J. D. Corbett, *Z. Anorg. Allg. Chem.* **1992**, *616*, 61.
[25] T. B. Massalski (Ed.): Binary Alloy Phase Diagrams. 2nd Ed., ASM International, Materials Park, Ohio 1990.
[26] a) T. Roisnel, J. Rodriguez-Carvajal, *WinPLOTR*, version May 2000: Materials Science Forum, Proceedings of the 7th European Powder Diffraction Conference 2000, Barcelona, Spain, p. 188 b) J. Rodriguez-Carvajal, *FULLPROF.2k*, version 1.6; 2000, Laboratoire Léon Brillouin: 2000. In Abstract of Satellite Meeting on Powder Diffraction, Congress of the International Union of Crystallography, Toulouse, France, 1990, p. 127.
[27] K. Koepernik, H. Eschrig, *Phys. Rev. B* **1999**, *59*, 1743.
[28] J. P. Perdew, Y. Wang, *Phys. Rev. B* **1992**, *45*, 13244.
[29] H. Eschrig: Optimized LCAO Method and the Electronic Structure of Extended Systems, Springer, Berlin, 1989.
[30] F. Merlo, M. L. Fornasini, *J. Less-Common Met.* **1967**, *13*, 603.
[31] G. Bruzzone, E. Franceschi, *J. Less-Common Met.* **1978**, *57*, 201.
[32] W. Dörrscheidt, A. Widera, H. Schäfer, *Z. Naturforsch.* **1977**, *32b*, 1097.
[33] N. E. Brese, M. O'Keeffe, *J. Solid State Chem.* **1990**, *87*, 134.
[34] U. Steinbrenner, A. Simon, *Z. Anorg. Allg. Chem.* **1998**, *624*, 228.
[35] M. Kirchner, W. Schnelle, F. R. Wagner, R. Niewa, *Solid State Sci.* **2003**, *5*, 1247.
[36] P. W. Selwood: Magnetochemistry, 2nd Ed., Interscience, New York 1956.
[37] D. S. Bem, C. M. Lampe-Önnerud, H. P. Olsen, H.-C. zur Loye, *Inorg. Chem.* **1996**, *35*, 581.
[38] D. S. Bem, H. P. Olsen, H.-C. zur Loye, *Chem. Mater.* **1995**, *7*, 1824.
[39] J. D. Houmes, S. Deo, H.-C. zur Loye, *J. Solid State Chem.* **1997**, *131*, 374.

